Stopband Performance Improvement of Rectangular Waveguide Filters Using Stepped-Impedance Resonators

Marco Morelli, Ian Hunter, Richard Parry, and Vasil Postoyalko

***Abstract*—Rectangular waveguide stepped-impedance resonators (SIRs) are analyzed and employed in the design of an X-band filter with center frequency $f_0 = 10$ GHz and a bandwidth of 100 MHz. An attenuation of 80 dB is held up to 23.1 GHz and, compared to standard uniform-impedance-resonator filters, a reduction in length of 55% is achieved at the expense of an increased insertion loss from 0.6 to 1.5 dB. The second resonance of the fundamental TE_{10} mode can be controlled by adjusting the length and impedance ratio of each resonator. A design procedure that takes into account step discontinuities is described and applied to the design of a number of SIR filters. Finally, the presented theory is supported with experimental results.**

***Index Terms*—Rectangular waveguides, stepped-impedance resonators, stopband improvement of filters, waveguide filters.**

I. Introduction

THE demand for microwave filters having better and better performances and low production costs is ever increasing in the fast-growing wireless communication markets. The development of new solutions is dictated by the need for more stringent requirements on both in-band and out-of-band performances: low loss, high selectivity, high rejection, wide spurious-free frequency ranges, and so forth. In particular, when out-of-band rejections are concerned, distributed microwave filters usually present unwanted spurious transmissions whose level might be unsatisfactory in some instances. In order to recover the required level of rejection, a low-pass filter is usually employed, leading to higher cost and complexity in the manufacture of microwave filters.

Unlike lumped-element bandpass filters where all resonant structures resonate at only one frequency, distributed bandpass filters have resonant structures that exhibit not one, but a number of resonances. The reasons for this are as follows:

- the fundamental mode of propagation of the guiding structure used to build the filter resonates when the electrical length of a resonator satisfies a certain resonance condition; due to the periodic nature of distributed elements, this condition yields more than one solution;
- as well as the fundamental mode, higher order modes are present and they show the same kind of unwanted resonances.

Manuscript received August 7, 2000; revised July 26, 2001.

The authors are with Filtronic Plc (U.K.), Leeds BD17 7SW, U.K. and also with the School of Electronic and Electrical Engineering, The University of Leeds, Leeds BD17 7SW, U.K.

Publisher Item Identifier 10.1109/TMTT.2002.800381.

A number of approaches have been proposed in order to reduce such spurious transmissions in microwave filters. As far as rectangular waveguide E-plane filters are concerned, improved stopband attenuation can be achieved by employing either wider or narrower resonators (or thicker inserts), depending on the position of the passband within the fundamental TE_{10} mode range [1]. Alternatively, ridged waveguide resonators can be employed [2]. However, these approaches can provide sufficient attenuation only up to frequencies around 1.4 times the center frequency of the filter. The use of multiple inserts [3] can extend the spurious-free frequency range up to half an octave (i.e., 1.5 times the center frequency), but it also leads to a higher degree of complexity.

Better stopband performance (attenuation up to $1.7f_0$) can be achieved by using inductive irises and resonators having different transversal dimensions [4], [5], so that they all resonate at the same fundamental frequency (the center frequency of the filter), but at different harmonic frequencies.

The use of stepped-impedance resonators (SIRs) [6] is based on the same principle and improved stopband performances of parallel coupled stripline filters [7] and comb-line filters [8]–[10] have been achieved.

In this paper, the resonant properties of SIRs are exploited in the design of rectangular waveguide filters with improved stopband performance. An accurate design procedure is outlined and a number of theoretical and experimental results are given.

II. Resonant Properties of SIRs

All resonant frequencies of a uniform-impedance resonator (UIR)are determined by the length of the resonator itself, which represents the only degree of freedom of the structure. In other words, the fundamental resonant frequency f_0 is controlled by the length of the resonator, but also all the higher resonant frequencies are fixed. If more degrees of freedom are added, then more resonant frequencies can be controlled.

In this paper, the interest will be focused on the ability to control the second resonance; hence, only one extra degree of freedom is required. For this purpose, the symmetrical SIR shown in Fig. 1 will be analyzed. The physical length l of each section and the ratio between the two impedances

$$K = \frac{Z_2}{Z_1} \tag{1}$$

are the two parameters that can be adjusted to control the fundamental and the second resonant frequencies.

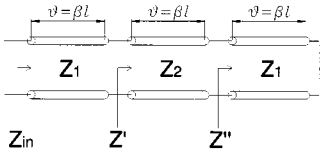

Fig. 1. SIR (ignoring step discontinuities).

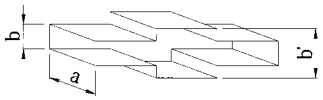

Fig. 2. Rectangular waveguide E-plane SIR ($Z_2/Z_1 = b'/b$).

As far as rectangular waveguide resonators are concerned, changes of impedance can be realized by E-plane or H-plane steps. For an H-plane SIR, the cutoff frequencies of the inner section and the outer sections are different. In order to keep the fundamental mode in propagation in each section while preventing the higher order modes from propagating at the center frequency of the filter, the ratio between the two broad dimensions is limited. As a consequence, the impedance ratio (1) is also restricted to a limited range. Indeed, for an E-plane SIR, this constraint does not hold and a wider range of impedance ratios is achievable. Hence, the interest will be focused on an E-plane SIR, which is shown in Fig. 2.

A. Ideal SIR

The effects of higher order modes excited at each impedance step will be neglected in this section. Under this condition, the expression for the input impedance of the resonator is

$$Z_{in} = Z_1 \frac{Z'' + jZ_1 \tan\vartheta}{Z_1 + jZ'' \tan\vartheta} \tag{2}$$

where

$$Z'' = Z_2 \frac{Z' + jZ_2 \tan\vartheta}{Z_2 + jZ' \tan\vartheta} \tag{3}$$

$$Z' = jZ_1 \tan\vartheta. \tag{4}$$

$\vartheta = \beta l$ is the electrical length of each section and β is the propagation constant of the fundamental mode.

It is easy to prove that the resonator shows a series resonance ($Z_{\rm in} = 0$) when ϑ and K satisfy the relation

$$K = \sqrt{1 + \tan^2\vartheta} - 1 \tag{5}$$

or

$$\vartheta = \pm\arctan\left(\sqrt{K(K+2)}\right) + n\pi, \qquad n = 0, 1, 2, \ldots. \tag{6}$$

By imposing the condition $\vartheta > 0$, it follows that the fundamental resonance is obtained when

$$\vartheta = \vartheta_0 = \arctan\left(\sqrt{K(K+2)}\right) \tag{7}$$

while the second resonance appears when

$$\vartheta = \vartheta_1 = \pi - \arctan\left(\sqrt{K(K+2)}\right) = \pi - \vartheta_0. \tag{8}$$

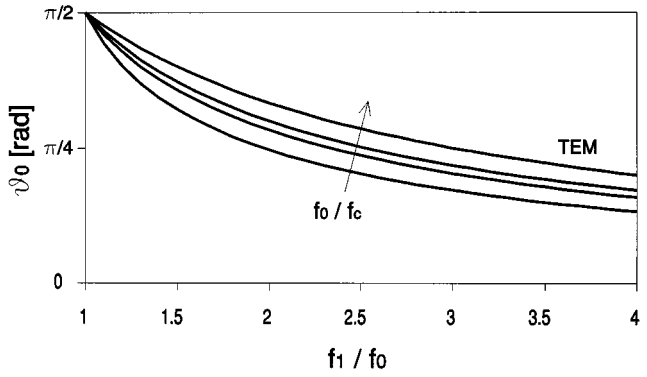

Fig. 3. Fundamental resonant electrical length for a TEM resonator ($f_c = 0$) and a waveguide resonator ($f_0/f_c = 1.25;\ 1.50;\ 1.75$).

The electrical lengths ϑ_0 and ϑ_1 are related by

$$\vartheta_1 = \beta(f_1)l = \frac{\beta(f_1)}{\beta(f_0)}\vartheta_0 \tag{9}$$

where f_0 and f_1 are the fundamental and second resonant frequencies, respectively. Therefore, by substituting (9) into (8), it follows that

$$\vartheta_0 = \frac{\pi}{1 + \frac{\beta(f_1)}{\beta(f_0)}} \tag{10}$$

and

$$K = \sqrt{1 + \tan^2\vartheta_0} - 1 = \sqrt{1 + \tan^2\left(\frac{\pi}{1 + \frac{\beta(f_1)}{\beta(f_0)}}\right)} - 1. \tag{11}$$

For waveguide resonators, the ratio $\beta(f_1)/\beta(f_0)$ can be written as

$$\frac{\beta(f_1)}{\beta(f_0)} = \sqrt{\frac{f_1^2 - f_c^2}{f_0^2 - f_c^2}} = \sqrt{\frac{\left(\frac{f_1}{f_0}\right)^2 - \left(\frac{f_c}{f_0}\right)^2}{1 - \left(\frac{f_c}{f_0}\right)^2}} \tag{12}$$

where f_c is the cutoff frequency of the fundamental $\rm TE_{10}$ mode.

By substituting (12) into (10) and (11), direct expressions for ϑ_0 and K in terms of f_0, f_1, and f_c are found.

The broad dimension of a waveguide resonator is usually chosen so that f_0 lies between $1.25f_c$ and $1.75f_c$. The plots shown in Figs. 3 and 4 illustrate the behavior of ϑ_0 and K as functions of the ratio f_1/f_0 for different values of f_0/f_c. The behavior for a TEM resonator is recovered with $f_c = 0$.

Conversely, given the physical length l and the ratio K, the resonant frequencies f_0 and f_1 can be easily determined by means of (7)–(9). Notice that (12) can be inverted to give a useful expression for the ratio f_1/f_0 as follows:

$$\frac{f_1}{f_0} = \sqrt{\left(\frac{\vartheta_1}{\vartheta_0}\right)^2\left[1 - \left(\frac{f_c}{f_0}\right)^2\right] + \left(\frac{f_c}{f_0}\right)^2}. \tag{13}$$

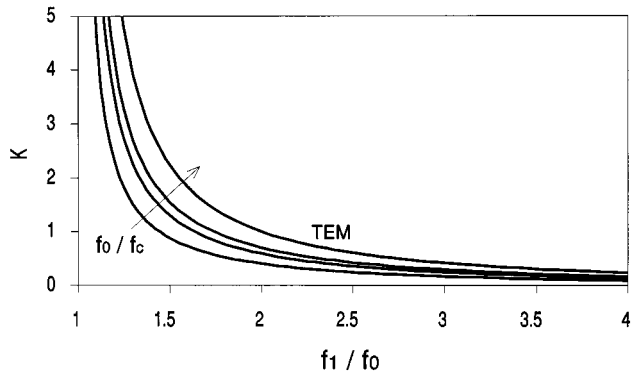

Fig. 4. Impedance ratio for a TEM resonator ($f_c = 0$) and a waveguide resonator ($f_0/f_c = 1.25;\ 1.50;\ 1.75$).

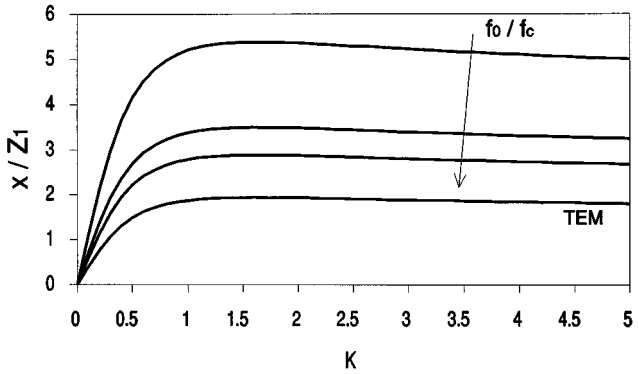

Fig. 5. Reactance slope parameter for a TEM resonator ($f_c = 0$) and a waveguide resonator ($f_0/f_c = 1.25;\ 1.50;\ 1.75$).

The reactance slope parameter [11] of the ideal SIR can be calculated by differentiating the expression for the input impedance to give

$$x = Z_1 \left(1 + \frac{1}{1+K}\right) f_0 \left.\frac{d\vartheta}{df}\right|_{f=f_0} \tag{14}$$

which for TEM resonators reduces to

$$x = Z_1 \left(1 + \frac{1}{1+K}\right) \vartheta_0 \tag{15}$$

while for waveguide resonators it becomes

$$x = Z_1 \left(1 + \frac{1}{1+K}\right) \frac{\vartheta_0}{1 - \left(\frac{f_c}{f_0}\right)^2}. \tag{16}$$

The behavior of the reactance slope parameter x as a function of K for different values of f_c/f_0 is illustrated in Fig. 5.

It is worth noting that, if $K = 1$, then the expressions for a UIR of total length 3ϑ are recovered, namely,

$$3\vartheta_0 = 3\arctan\left(\sqrt{3}\right) = \pi \tag{17}$$

$$3\vartheta_1 = 3\left[\pi - \arctan\left(\sqrt{3}\right)\right] = 2\pi \tag{18}$$

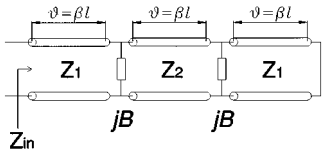

Fig. 6. SIR (including step discontinuities).

and

$$x = Z_1 \frac{\pi}{2} \quad \text{(TEM resonators)} \tag{19}$$

$$x = Z_1 \frac{\pi}{2} \frac{1}{1 - \left(\frac{f_c}{f_0}\right)^2} \quad \text{(waveguide resonators)}. \tag{20}$$

Also, (13) becomes

$$\frac{f_1}{f_0} = \sqrt{4\left[1 - \left(\frac{f_c}{f_0}\right)^2\right] + \left(\frac{f_c}{f_0}\right)^2} = \sqrt{4 - 3\left(\frac{f_c}{f_0}\right)^2}. \tag{21}$$

From the plots shown, it follows that a value of $K > 1$ will result in a lower second resonant frequency f_1 compared to a standard UIR [i.e., a ratio f_1/f_0 smaller than (21)]. Vice versa, a wider separation between the fundamental and the second resonances will be achieved with a value $K < 1$; in this case, the length of the resonator will reduce, but the reactance slope parameter x will decrease, leading to a smaller Q factor and an increased insertion loss.

B. Practical SIR

The expressions for the resonance condition and the reactance slope parameter derived above are not rigorously valid, because of the inevitable presence of higher order modes excited at each impedance step.

For frequencies such that all higher order modes are below cutoff, their effects can be modeled by shunt susceptances as shown in Fig. 6 In this case, the resonant condition $Z_{\text{in}} = 0$ gives

$$K = \frac{\sqrt{1 + \tan^2\vartheta} - 1}{1 - \overline{B}\tan\vartheta} \tag{22}$$

or

$$\vartheta = \arctan\left(\frac{D \pm E}{F}\right) + n\pi, \qquad n = 0,\ 1,\ 2,\ \ldots \tag{23}$$

where $\overline{B}$ is the susceptance associated with each step normalized to $Y_1 = 1/Z_1$ and D, E, and F are given by

$$D = \overline{B}K(K+1) \tag{24}$$

$$E = \sqrt{K\left[K\left(\overline{B}^2 + 1\right) + 2\right]} \tag{25}$$

$$F = \left(\overline{B}K + 1\right)\left(\overline{B}K - 1\right). \tag{26}$$

Again, by imposing the condition $\vartheta > 0$, it can be proved that the fundamental resonance is given by

$$\vartheta = \vartheta_0 = \arctan\left(\frac{D_0 - E_0}{F_0}\right) \tag{27}$$

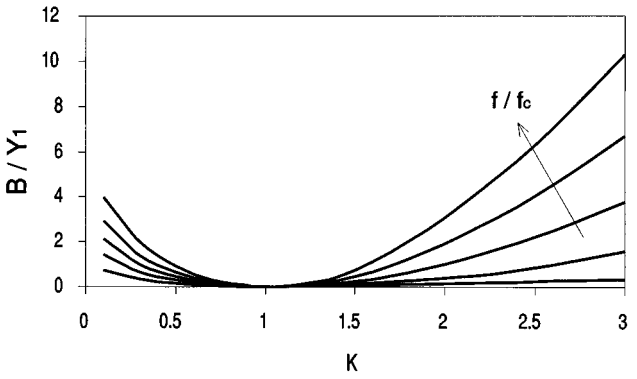

Fig. 7. Normalized susceptance of a waveguide E-plane step ($f/f_c = 1.25$; 1.75; 2.25; 2.75; 3.25).

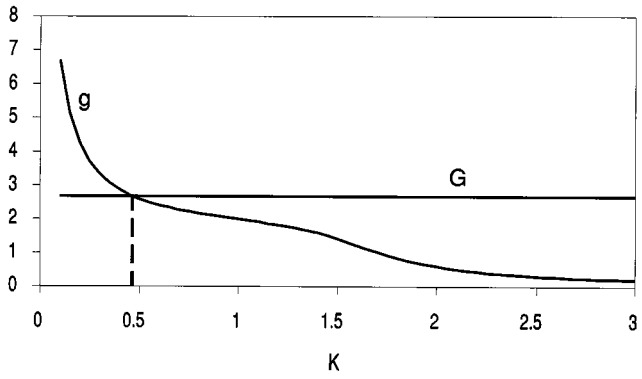

Fig. 8. Graphical solution of (31) with $f_1/f_0 = 2.1$ and $f_0/f_c = 1.5$.

and the second resonance is obtained when

$$\vartheta = \vartheta_1 = \begin{cases} \arctan\left(\dfrac{D_1 + E_1}{F_1}\right), & \text{if } \overline{B}K > 1 \\ \arctan\left(\dfrac{D_1 + E_1}{F_1}\right) + \pi, & \text{if } \overline{B}K < 1. \end{cases} \tag{28}$$

Note that $\overline{B}$ is a function of the ratio K and also varies with frequency, as shown in Fig. 7 for a waveguide E-plane step.[1] Therefore, the coefficients D, E, and F are also frequency-dependent. As a consequence, direct expressions providing l and K as functions of f_0 and f_1 do not exist. In a later section, an iterative algorithm suitable for numerical implementation will be presented; however, the unknown parameters l and K can be derived by a graphical method as follows.

Once the values for the susceptance $\overline{B}$ as a function of K and f/f_c are available (as in Fig. 7), it is possible to calculate $\vartheta_0(K)$ (evaluated at $f/f_c = f_0/f_c$) and $\vartheta_1(K)$ (evaluated at $f/f_c = f_1/f_c$) by means of (24)–(28). Then, from (12) (which is still valid), it follows that the ratio

$$g(K)_{f_0/f_c,\, f_1/f_c} = \frac{\vartheta_1(K)_{f_1/f_c}}{\vartheta_0(K)_{f_0/f_c}} \tag{29}$$

must assume the known value

$$G = \sqrt{\frac{\left(\frac{f_1}{f_0}\right)^2 - \left(\frac{f_c}{f_0}\right)^2}{1 - \left(\frac{f_c}{f_0}\right)^2}}. \tag{30}$$

Now the equation

$$g(K)_{f_0/f_c,\, f_1/f_c} = G \tag{31}$$

can be solved graphically to provide the required value K as shown in Fig. 8. Then, ϑ_0 can be determined by (27), from which $l = \vartheta_0/\beta(f_0)$.

When the reactance slope parameter is considered, it can be proved that

$$x = Z_1 \left(1 + \frac{1}{K} - \frac{1}{K\sqrt{1 + \tan^2 \vartheta_0}}\right) f_0 \left.\frac{d\vartheta}{df}\right|_{f=f_0} \tag{32}$$

if $d\overline{B}/df$ is assumed to be negligible.

[1]This data has been extrapolated from [12].

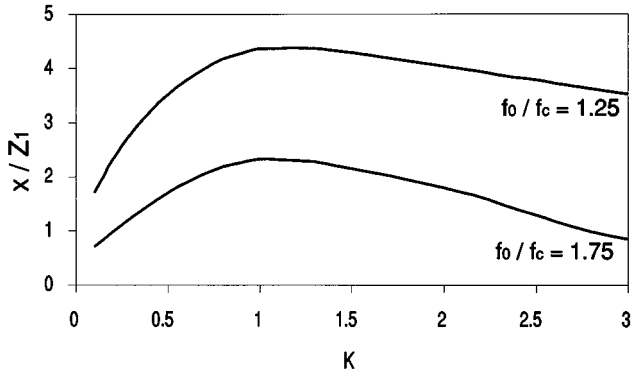

Fig. 9. Reactance slope parameter for a waveguide SIR.

Again, for TEM resonators, the above expression reduces to

$$x = Z_1 \left(1 + \frac{1}{K} - \frac{1}{K\sqrt{1 + \tan^2 \vartheta_0}}\right) \vartheta_0 \tag{33}$$

and for waveguide resonators it is

$$x = Z_1 \left(1 + \frac{1}{K} - \frac{1}{K\sqrt{1 + \tan^2 \vartheta_0}}\right) \frac{\vartheta_0}{1 - \left(\frac{f_c}{f_0}\right)^2} \tag{34}$$

which is plotted in Fig. 9. Once again, when a bigger f_1/f_0 is required, (12) and the plot in Fig. 8 indicate that a value of $K < 1$ is required, while for a smaller f_1/f_0 a value of $K > 1$ is needed. In both cases, the reactance slope parameter is reduced. Also, the length of the resonator is reduced or increased if $K < 1$ or $K > 1$, respectively.

III. Design

The stopband performance of microwave filters can be improved by employing SIRS because of the ability to control spurious resonances. All resonators must of course have the fundamental resonance at the center frequency f_0 of the filter; however, they can be designed to have different second resonant frequencies $f_1^{(1)}$, $f_1^{(2)}$, …, $f_1^{(n)}$, where the superscript (i) designates the ith resonator. In this way, the second passband arising around $\hat{f}_1$ will[2] be spread over the frequency range between the minimum and the maximum of $\{f_1^{(i)}\}$ approximately; the bigger

[2]Frequency $\hat{f}_1$ is the second resonant frequency of a UIR with the fundamental resonance at f_0; the ratio $\hat{f}_1/f0$ is given by (21).

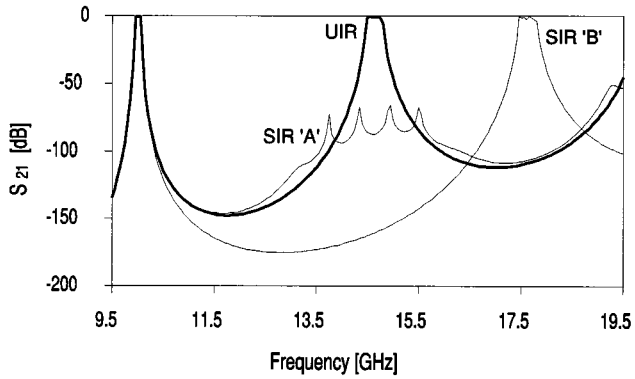

Fig. 10. Calculated stopband performance of UIR versus SIR filters.

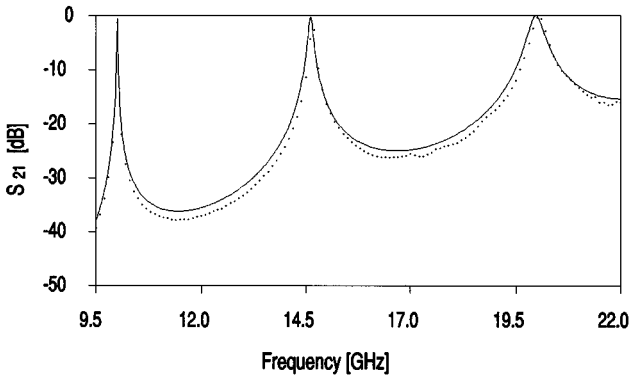

Fig. 11. Predicted (solid) and measured (•) transmission of the single-section UIR filter.

this range, the lower the level of the resonances and the better the stopband performance of the filter.

Alternatively, it is possible to design the filter by using resonators with the same second resonant frequency f_1, provided that this frequency is chosen far away from any frequency range where good attenuation is required.

These two ideas are illustrated in Fig. 10, where the simulated response of three six-section filters ($f_0 = 10$ GHz) is shown. The resonators of filter *SIR* A were designed to have different second resonant frequencies equally distributed over the range $[\hat{f}_1 - 1.5$ GHz, $\hat{f}_1 + 1.5$ GHz]; while the common second resonant frequency of the resonators of filter SIR, B was chosen to be $\hat{f}_1 + 3$ GHz.

The filters shown in the next sections employ rectangular waveguide SIRs coupled by symmetric inductive irises. The electrical design was based on a Chebychev response with a maximum return loss of 25 dB.

A. Resonator

An iterative algorithm was developed to obtain the values for ϑ_0 and K in the presence of step discontinuities. Given f_0 and f_1, the initial values for ϑ_0 and K are determined by means of (10) and (11), which hold for the ideal case. Then the susceptance $\overline{B}$ is evaluated at both frequencies f_0 and f_1

$$\overline{B_0} = \overline{B}(K, f_0) \qquad \overline{B_1} = \overline{B}(K, f_1) \tag{35}$$

and the coefficients D_0, E_0, F_0, D_1, E_1, and F_1 are determined by means of (24)–(26).

Then, based on (27), (28), and (9), two intermediate values $\vartheta^{(a)}$ and $\vartheta^{(b)}$ are calculated as

$$\vartheta^{(a)} = \arctan\left(\frac{D_0 - E_0}{F_0}\right) \tag{36}$$

and

$$\vartheta^{(b)} = \frac{\beta(f_0)}{\beta(f_1)} \times \begin{cases} \arctan\left(\dfrac{D_1 + E_1}{F_1}\right), & \text{if } \overline{B_1}K > 1 \\ \arctan\left(\dfrac{D_1 + E_1}{F_1}\right) + \pi, & \text{if } \overline{B_1}K < 1. \end{cases} \tag{37}$$

If $\vartheta^{(a)}$ and $\vartheta^{(b)}$ differ by an amount greater than a predetermined accuracy ϵ, then the following steps take place.

If $\vartheta^{(a)} < \vartheta^{(b)}$, K is increased by a predetermined quantity ΔK; whilst if $\vartheta^{(a)} > \vartheta^{(b)}$, K is decreased by ΔK. With this new value of K, the susceptances $\overline{B_0}$ and $\overline{B_1}$ and the coefficients D, E, and F are evaluated again together with $\vartheta^{(a)}$ and $\vartheta^{(b)}$ and the cycle is repeated until $|\vartheta^{(a)} - \vartheta^{(b)}| < \epsilon$. Eventually, ϑ_0 and K will be set to

$$\vartheta_0 = \vartheta^{(a)} \tag{38}$$

and

$$K = \frac{\sqrt{1 + \tan^2 \vartheta_0} - 1}{1 - \overline{B_0} \tan \vartheta_0}. \tag{39}$$

The reactance slope parameter x is given by (34). It can be proved that if ΔK is chosen to be sufficiently small, then the convergence of the algorithm is guaranteed.

IV. Results

A. Single-Section SIR Filters

A single-section UIR filter was designed with the fundamental resonance at $f_0 = 10$ GHz and a bandwidth of 1 MHz. In order to validate the design procedure and also evaluate the impact on the Q factor, the algorithm described above was used to design two single-section SIR filters with the same fundamental resonance and bandwidth and the second resonant frequencies at $f_1^a = 13.15$ GHz and $f_1^b = 21.65$ GHz, respectively.

The algorithm provides the values $K_a = 1.50$, $\vartheta_a = 1.12$ and $K_b = 0.32$, $\vartheta_b = 0.64$. Notice that, for the UIR filter, (10) gives $\vartheta = \pi/3 = 1.05$; therefore, the relative lengths of the SIR filters compared to the UIR filter are $\vartheta_a/\vartheta = 107\%$ and $\vartheta_b/\vartheta = 61\%$, respectively. The simulated and measured responses of the three filters are shown in Figs. 11–13. The measurements for the Q factor[3] and the insertion loss at resonance are summarized in Table I. Notice that the wider stopband and the reduced length of filter b are obtained at the expense of an increased insertion loss by a factor 2.

B. Six-Section SIR Filters

A number of six-section filters with center frequency $f_0 = 10$ GHz and a bandwidth of 100 MHz were designed and realized by employing UIRs and SIRs. A WR75 realization was

[3]The predicted Q factor [13] of a WR75 copper resonator is approximately 7520 at 10 GHz, which means a practical value of about 5300.

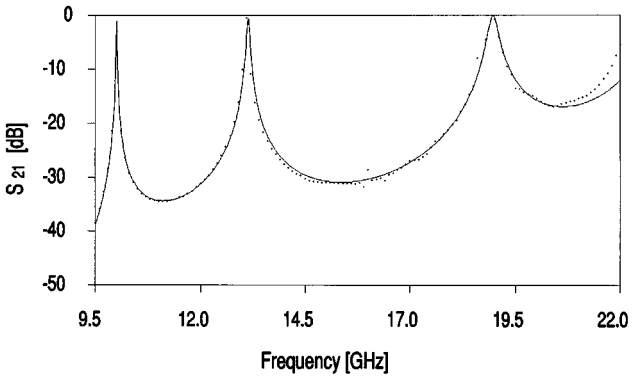

Fig. 12. Predicted (solid) and measured (•) transmission of single-section SIR filter a.

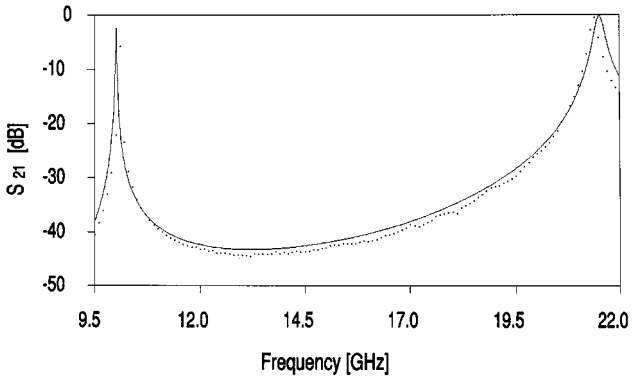

Fig. 13. Predicted (solid) and measured (•) transmission of single-section SIR filter b.

TABLE I
CALCULATED Q FACTOR AND MEASURED INSERTION LOSS

Filter	Q	I.L.
UIR	5370	-0.84 dB
SIR a	5840	-0.74 dB
SIR b	2330	-1.75 dB

chosen so that the second resonance of the fundamental mode for the UIR filter occurred within the fundamental mode range (7.869–15.737 GHz) at approximately

$$\hat{f}_1 = \sqrt{4f_0^2 - 3f_c^2} = 14.65 \text{ GHz}. \tag{40}$$

The simulation and the measurement of the UIR filter transmission are shown in Fig. 14. The measured insertion loss at the mid-band frequency was 0.6 dB. Notice that an attenuation of 50 dB was held up to 14.2 GHz, that is, up to $1.42f_0$.

The first SIR filter (filter A) was designed with three resonators having the second resonant frequency at

$$f_1^{(1)} = f_1^{(2)} = f_1^{(3)} = f_1^a = 13.1 \text{ GHz} \tag{41}$$

and three resonators with

$$f_1^{(4)} = f_1^{(5)} = f_1^{(6)} = f_1^b = 16.2 \text{ GHz}. \tag{42}$$

In this way, the three resonant frequencies f_0, f_1^a, and f_1^b were equally spaced and also f_1^a and f_1^b were symmetrically placed around $\hat{f}_1$. The simulation and the measurement are shown in Fig. 15. An insertion loss of 0.7 dB was measured at the center

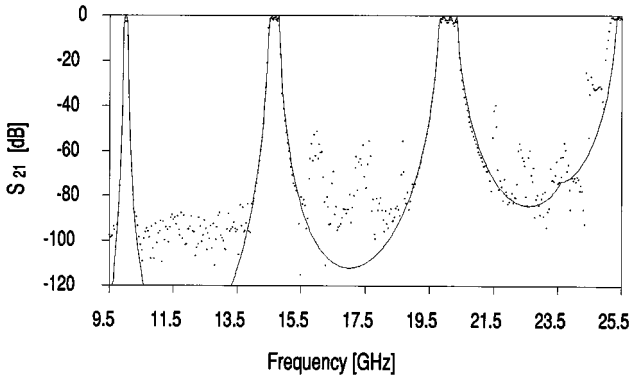

Fig. 14. Predicted (solid) and measured (•) transmission of the UIR filter.

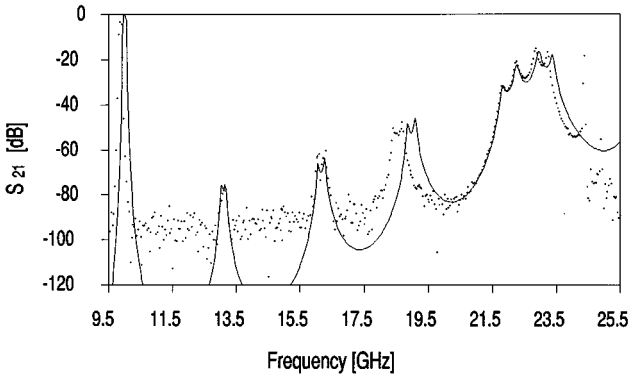

Fig. 15. Predicted (solid) and measured (•) transmission of SIR filter A.

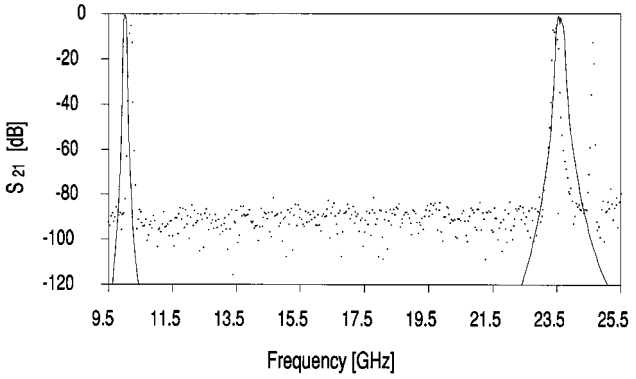

Fig. 16. Predicted (solid) and measured (•) transmission of SIR filter B.

frequency of the filter. In this case, an attenuation of 50 dB was provided up to 18.2 GHz, that is, up to $1.82f_0$; moreover, 45 dB of attenuation was maintained up to 21.5 GHz, which is a frequency range more than one octave wide.

The second SIR filter (filter B) was designed with all six resonators having the re-resonance pushed beyond the cutoff frequency of the TE_{30} mode, i.e., at

$$f_1^{(i)} = \hat{f}_1 + 9 \text{ GHz} = 23.65 \text{ GHz}, \qquad i = 1, 2, \ldots 6. \tag{43}$$

Since symmetric irises were used, the TE_{20} mode was not excited and a very good attenuation of 80 dB was held over a wide frequency range up to 23.1 GHz, as shown in Fig. 16. Surprisingly, even when the TE_{20} mode was deliberately excited, the response remained virtually unchanged, as shown in Fig. 17, where the transmission of this filter is compared

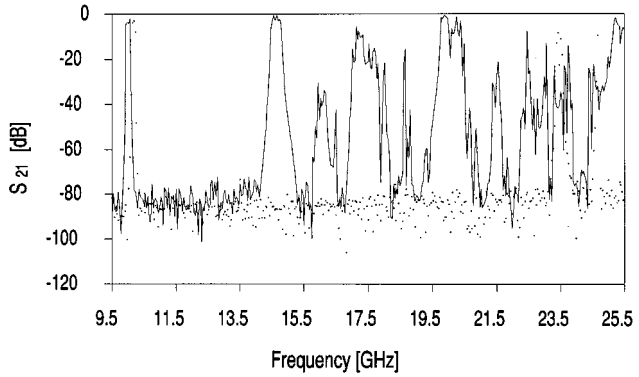

Fig. 17. Measured transmission of SIR filter B (•) and UIR filter (solid) with displaced flanges.

TABLE II
PHYSICAL DIMENSIONS OF SIR FILTER B

	d [mm]	$l1$ [mm]	$l2$ [mm]	$l3$ [mm]	$b2$ [mm]
1	7.66	2.89	4.35	4.10	2.38
2	3.58	4.10	4.35	4.17	2.38
3	3.12	4.17	4.35	4.18	2.38
4	3.05	4.18	4.35	4.17	2.38
5	3.12	4.17	4.35	4.10	2.38
6	3.58	4.10	4.35	2.89	2.38
7	7.66				

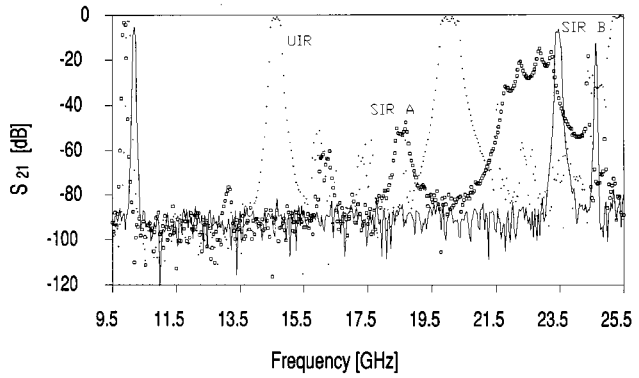

Fig. 18. UIR versus SIR filters' measured transmission.

to the UIR filter when both input and output flanges were displaced by 5 mm along the broad dimension. The physical dimensions of this filter are reported in Table II, where the first column (d) contains the apertures of each coupling iris, $l1$ and $l3$ are the lengths of the outer sections of each resonator, while $l2$ and $b2$ are the length and the height of the inner sections, respectively. The heights $b1$ and $b3$ of the outer sections were 9.53 mm (WR75 narrow dimension). The common width a was 19.05 mm (WR75 broad dimension) and the iris thickness was 0.50 mm. The measured insertion loss at the mid-band frequency was 1.5 dB, which is in accordance with the previous discussion on the Q factor degradation. Also, it should be noted that the length of the filter was considerably reduced to about 55% of the UIR filter length.

The improved performance of the presented filters is evident in Fig. 18, where the measured response of the UIR filter is directly compared to the measured responses of SIR filters A and B.

V. CONCLUSION

The use of SIRs has been extended to the design of rectangular waveguide bandpass filters in this paper. Compared to standard UIR filters, a better stopband performance is clearly achieved. Also, a significant reduction in size can be obtained at the expense of an increased insertion loss. An accurate design procedure that takes into account the effects of impedance steps has been presented and used to design and realize a number of SIR filters. Theoretical and experimental performances of two of these filters have been compared to standard UIR filter performances and the good agreement between theory and experiment validates the design procedure.

A common way of realizing a UIR filter with inductive irises is to assemble a main body (with all the cavities and the irises) and a straight cover. In order to realize an SIR filter, steps are added to the main body and to the cover. The incremental cost of realizing an SIR filter is mainly due to the steps of the cover, as the steps inside the main body do not add any extra features to be machined out compared to a UIR filter. This cost is significantly lower than the cost incurred by making and assembling a low-pass filter to an UIR filter, although the low-pass filter usually provides attenuation at the third and fourth harmonic frequencies also. Moreover the presented SIR filter suffers from a reduced power handling capability due to the narrower section of each resonator. However, in those low-power applications where the use of an SIR filter would meet the stopband specification without the need for a low-pass filter while keeping the insertion loss within the required limit, the SIR filter indeed represents a cost-effective solution.

In any case, SIRs provide the designer with an extra degree of freedom to exploit in order to achieve the best compromise in terms of insertion loss, stopband, size, and cost.

ACKNOWLEDGMENT

The authors wish to thank Prof. J. D. Rhodes, Filtronic Plc (U.K.), Leeds, U.K., and P. Geraghty, Filtronic Plc (U.K.), Leeds, U.K., for the helpful discussions and suggestions and also all the staff at Filtronic Comtek (U.K.) involved in the realization of the filters. Particular mention also goes to one of the unknown reviewers whose comments contributed to a remarkable improvement of this paper.

REFERENCES

[1] F. Arndt, J. Bornemann, R. Vahldieck, and D. Grauerholz, "E-plane integrated circuit filters with improved stopband attenuation," *IEEE Trans. Microwave Theory Tech.*, vol. MTT-32, pp. 1391–1394, Oct. 1984.

[2] D. Budimir, "Optimized E-plane bandpass filters with improved stopband performance," *IEEE Trans. Microwave Theory Tech.*, vol. 45, pp. 212–220, Feb. 1997.

[3] R. Vahldieck and W. J. R. Hoefer, "Finline and metal insert filters with improved passband separation and increased stopband attenuation," *IEEE Trans. Microwave Theory Tech.*, vol. MTT-33, pp. 1333–1339, Dec. 1985.

[4] H. J. Riblet, "Waveguide filter having nonidentical sections resonant at same fundamental frequency and different harmonic frequencies," U.S. Patent 3 153 208, Oct. 1964.

[5] M. Morelli, I. Hunter, R. Parry, and V. Postoyalko, "Stop-band improvement of rectangular waveguide filters using different width resonators: Selection of resonator widths," in *IEEE MTT-S Int. Microwave Symp. Dig.*, Phoenix, AZ, May 2001, pp. 1623–1626.

[6] M. Sagawa, M. Makimoto, and S. Yamashita, "Geometrical structures and fundamental characteristics of microwave stepped-impedance resonators," *IEEE Trans. Microwave Theory Tech.*, vol. 45, pp. 1078–1085, July 1997.
[7] M. Makimoto and S. Yamashita, "Bandpass filters using parallel coupled stripline stepped impedance resonators," *IEEE Trans. Microwave Theory Tech.*, vol. MTT-28, pp. 1413–1417, Dec. 1980.
[8] ——, "Compact bandpass filters using stepped impedance resonators," *Proc. IEEE*, vol. 67, pp. 16–19, Jan. 1979.
[9] M. Sagawa, M. Makimoto, and S. Yamashita, "A design method of bandpass filters using dielectric-filled coaxial resonators," *IEEE Trans. Microwave Theory Tech.*, vol. MTT-33, pp. 152–157, Feb. 1985.
[10] H. Yao, K. A. Zaki, and A. E. Atia, "Improvement of spurious performance of combline filters," in *IEEE MTT-S Int. Microwave Symp. Dig.*, Denver, CO, June 1997, pp. 1099–1102.
[11] G. L. Matthaei, L. Young, and E. M. T. Jones, *Microwave Filters, Impedance-Matching Networks and Coupling Structures*. Norwood, MA: Artech House, 1980.
[12] N. Marcuvitz, *Waveguide Handbook*. New York: McGraw-Hill, 1951.
[13] S. Ramo, J. R. Whinnery, and T. Van Duzer, *Fields and Waves in Communication Electronics*, 2nd ed. New York: Wiley, 1984.

Marco Morelli was born in Italy in 1971. He received the Laurea degree (*summa cum laude*) in electronic engineering from the University of Ancona, Ancona, Italy, in 1996, and is currently working toward the Ph.D. degree at the School of Electronic and Electrical Engineering, The University of Leeds, Leeds, U.K.

In 1997, he joined Filtronic Plc, Leeds, U.K., where he is currently a Waveguide Design Engineer.

Ian Hunter graduated from The University of Leeds, Leeds, U.K., in 1978 and received the Ph.D. degree in 1981.

He is a Fellow Engineer with Filtronic Plc, Leeds, U.K., where he is currently employed on filter technologies for future cellular radio systems. He is also a Part-Time Senior Research Fellow with the Institute of Microwaves and Photonics, The University of Leeds, and has authored or co-authored over 50 technical papers on microwave and millimeter-wave filters and circuit theory. He recently authored *Theory and Design of Microwave Filters* for the IEE Electromagnetic Wave Series. He holds three patents.

Richard Parry received the B.Sc. degree (with first-class honors) in electrical and electronic engineering and the Ph.D. degree from The University of Leeds, Leeds, U.K., in 1979 and 1984, respectively.

He joined Filtronic Components Ltd., Leeds, U.K., in 1982 working on microwave filters and multiplexers. In 1983, he was employed by K. W. Engineering Inc., San Diego, CA, before returning to Filtronic in 1985, where he was responsible for developing extensive CAD software for the design, simulation, and optimization of microwave filters and multiplexers realized in SSS, waveguide, and combline structures. He is currently Technical Director of Filtronic Components Ltd., which is now part of the Electronic Warfare Division of Filtronic Plc. In 1997, he joined the Institute of Microwaves and Photonics, The University of Leeds, where he is currently a Part-Time Senior Research Fellow.

Vasil Postoyalko was born in Leeds, U.K. He received the B.Sc. degree in mathematics and the Ph.D. degree in electronic engineering and applied mathematics from The University of Leeds, Leeds, U.K., in 1978 and 1985, respectively.

In 1983, he became a Research Engineer in the School of Electronic and Electrical Engineering, The University of Leeds, and since 1986 he has been a Lecturer. He is a member of the Institute of Microwaves and Photonics, The University of Leeds. His current research interest is in the design of microwave circuits.